Quantum fluctuations for two-level atoms in a high-Q cavity with a spatially varying field mode

Min Xiao and H. J. Kimble
Department of Physics, University of Texas at Austin, Austin, Texas 78712-9990

H. J. Carmichael
Department of Physics, University of Arkansas, Fayetteville, Arkansas 72701
(Received 17 December 1986)

An extension of the quantum theory of the atom-field interaction within a high-finesse resonator is made to include spatial variations of the field mode in the limit of small cavity decay rate. The two particular examples of a Gaussian mode field in a ring cavity and a plane-wave field in a standing-wave interferometer are presented to illustrate the method. Analytic expressions are obtained for the incoherent intensity and photon correlations of the transmitted field. In qualitative terms, effects such as sub-Poissonian photon statistics predicted by the plane-wave theory in a ring cavity are preserved. In either the weak-field or dispersive limit the results of the plane-wave theory in a ring cavity are recovered independent of the form of the spatial dependence of the cavity mode.

I. INTRODUCTION

In recent years several quantum statistical treatments of optical bistability have been developed for the system of homogeneously broadened two-level atoms interacting with a single damped cavity field mode. Extensive reviews of this subject can be found in the work of Lugiato[1] and of Carmichael.[2] In broad outline these theories deal with the coherent coupling of a collection of atoms to a high-finesse interferometer mode. Dissipation enters through the radiative decay of the atoms and the damping of the cavity. Steady-state operation is achieved with external excitation in the form of a coherent driving field. The interplay of the nonlinear deterministic dynamics and the quantum fluctuations about steady state gives rise to a diversity of phenomena. Of particular interest are such nonclassical effects as sub-Poissonian photon statistics, photon antibunching, and squeezing, which arise from the nonclassical nature of the fluctuations.

All of the theories of the quantum processes in optical bistability consider a plane-wave field mode in a ring cavity, which is not realistic in many experimental situations. The purpose of this paper is to extend these quantum statistical theories to include spatial variations of the field mode. Our work follows closely that of Drummond and Walls,[3] hereafter referred to as OBII, and is likewise carried out in the "good-cavity" limit, with cavity decay rate much smaller than either the atomic decay rates ($\gamma_\perp,\gamma_\parallel$) or the cavity coupling coefficient ($\sqrt{N}g$). We deal with the nonuniformity of the cavity field by dividing the cavity mode into small sections which are each microscopically large in terms of atomic number to allow truncation of the generalized Fokker-Planck equation, but which are macroscopically small to justify the assumption of constant field amplitude.

In Sec. II we obtain the linearized Fokker-Planck equation, and, from that, expressions for the ratio of incoherent intensity to coherent intensity and for the fourth-order field correlation function which describes sub-Poissonian photon statistics. In Secs. III and IV we present two examples to show how this theory applies to more realistic physical systems, namely, to a Gaussian field inside a ring cavity and to a plane wave inside a standing-wave interferometer. The results are illustrated with a number of figures for comparison with the existing literature on the plane-wave ring cavity. Section V serves as a summary of our findings.

II. MODEL AND LINEARIZED THEORY

We consider a single, quantized, spatially varying cavity mode interacting with a collection of homogeneously broadened two-level atoms. The atoms and the cavity are damped through coupling to reservoirs, and the cavity is driven by a coherent field of amplitude $\mathscr{E}$. We divide the cavity mode into M small sections with $N_j \gg 1$ atoms in the jth sector. Each section is assumed to be sufficiently small so that we can view the field as effectively constant across it. By following a procedure similar to that in OBII, using the electric dipole, rotating-wave, and Markovian[4] approximations, we find the quantum master equation can be written as

$$\frac{d\hat{\rho}}{dt}=\frac{1}{i\hbar}\left[\hbar\omega_c[\hat{a}^\dagger\hat{a},\hat{\rho}]+\tfrac{1}{2}\hbar\omega_a\sum_{j=1}^{M}[\hat{J}^z_j,\hat{\rho}]\right]+\sum_{j=1}^{M}(g_j[\hat{a}^\dagger\hat{J}^-_j,\hat{\rho}]-g_j[\hat{a}\hat{J}^+_j,\hat{\rho}])$$
$$+\sum_{j=1}^{M}\left[(\tfrac{1}{2}\gamma_\parallel)\sum_{i=1}^{N_j}([\hat{\sigma}^-_{ij}\hat{\rho},\sigma^+_{ij}]+[\hat{\sigma}^-_{ij},\hat{\rho}\hat{\sigma}^+_{ij}])+(\tfrac{1}{4}\gamma_p)\sum_{i=1}^{N_j}([\hat{\sigma}^z_{ij}\hat{\rho},\hat{\sigma}^z_{ij}]+[\hat{\sigma}^z_{ij},\hat{\rho}\hat{\sigma}^z_{ij}])\right]$$
$$+\kappa([\hat{a}\hat{\rho},\hat{a}^\dagger]+[\hat{a},\hat{\rho}\hat{a}^\dagger])+\kappa(\mathscr{E}e^{-i\omega_I t}[\hat{a}^\dagger,\hat{\rho}]-\mathscr{E}^*e^{i\omega_I t}[\hat{a},\hat{\rho}])\,. \tag{1}$$

Here ω_c is the cavity resonance frequency and ω_a is the atomic resonance frequency. $\mathscr{E}$ is the coherent driving field of frequency ω_I. g_j is the coupling coefficient between the cavity field mode and atoms in the jth section, and is given in terms of the normalized mode function $U(\mathbf{r}_j)$ by[5]

$$g_j=\left[\frac{\mu^2\omega_c}{2\hbar\varepsilon_0}\right]^{1/2}|U(\mathbf{r}_j)|\equiv g_0|U(\mathbf{r}_j)| \ . \tag{2}$$

It is precisely the spatial dependence of g_j that distinguishes the present calculation from the plane-wave theory, in which $g_j=g_0/\sqrt{V}$, with V the cavity volume. κ is the cavity damping rate, $\gamma_{||}$ is the Einstein A coefficient for spontaneous emission, and γ_p is the rate of collision-induced phase decay, which is related to the total rate of decay of the atomic polarization $\gamma_\perp$ by $\gamma_\perp=\gamma_p+\frac{1}{2}\gamma_{||}$. We set the thermal photon number in both the atomic and cavity-mode reservoirs to zero. The operators $\hat{a},\hat{a}^\dagger$ are the usual single-mode raising and lowering operators, and $\hat{\sigma}^z_{ij},\hat{\sigma}^\pm_{ij}$ are the Pauli operators for the ith atom of the jth section. The operators $\hat{J}^\pm_j,\hat{J}^z_j$ are cooperative operators for the jth section defined by

$$\hat{J}^\pm_j\equiv\sum_{i=1}^{N_j}e^{\pm i\eta(\mathbf{r}_{ij})}\hat{\sigma}^\pm_{ij} \ , \qquad \hat{J}^z_j\equiv\sum_{i=1}^{N_j}\hat{\sigma}^z_{ij} \ , \tag{3}$$

where $\eta(\mathbf{r}_{ij})$ expresses the phase variation within the sector [e.g., for the plane-wave ring, $\eta(\mathbf{r}_{ij})=\mathbf{k}\cdot\mathbf{r}_{ij}$]. Collective atomic operators for the same section obey the usual angular-momentum commutation relations while those for different sections commute.

We employ standard techniques[1-3,6,7] to transform the operator master equation (1) into a c-number generalized Fokker-Planck equation. The procedure involves an association between the density operator $\hat{\rho}$ and a quasiprobability distribution P, where the correspondence between complex c-numbers and quantum operators is as follows:

$$(J_j^-,J_j^+,J_j^z,\alpha^\dagger,\alpha)\leftrightarrow(\hat{J}_j^-,\hat{J}_j^+,\hat{J}_j^z,\hat{a}^\dagger,\hat{a}) \ . \tag{4}$$

We adopt a normal ordering scheme so that equal-time expectation values of normally ordered atomic and field variables are given by phase-space averages with respect to the distribution P; for example,

$$\mathrm{tr}(\hat{\rho}\hat{J}_i^+\hat{J}_j^z\hat{J}_k^-\hat{a}^\dagger\hat{a})=\int d^2\{J^+\}\int d^2\{J^z\}\int d^2\{J^-\}\int d^2\alpha^\dagger\int d^2\alpha\, P(\{J^+\},\{J^z\},\{J^-\},\alpha^\dagger,\alpha)J_i^+J_j^zJ_k^-\alpha^\dagger\alpha \ , \tag{5}$$

with a suitable generalization to higher-order moments and to unequal-time expectation values.[1-3,6,7] Since it is known that the Fokker-Planck equation derived using the Glauber-Sudarshan-Haken representation does not have positive-definite-diffusion,[4] we interpret P as a distribution in the positive P representation.[8] Equation (4) associates five independent complex variables with the quantum-mechanical operators, and the integration in (5) covers the entire $3M+2$ dimensions complex space.

By requiring a sufficient number of atoms in each of the M microscopic sections to allow truncation of the generalized Fokker-Planck equation to second order (basically a requirement on the smoothness of P over the inversion variables J_j^z), we arrive at the following Fokker-Planck equation:

$$\begin{aligned}\frac{\partial P(\boldsymbol{\alpha},t)}{\partial t}=&\left[-\frac{\partial}{\partial\alpha}\left[\kappa\mathscr{E}-\kappa'\alpha+\sum_{j=1}^{M}g_jJ_j^-\right]-\frac{\partial}{\partial\alpha^\dagger}\left[\kappa\mathscr{E}^*-\kappa^{*\prime}\alpha^\dagger+\sum_{j=1}^{M}g_jJ_j^+\right]\right.\\&-\sum_{j=1}^{M}\left[\frac{\partial}{\partial J_j^-}(g_j\alpha J_j^z-\gamma J_j^-)+\frac{\partial}{\partial J_j^+}(g_j\alpha^\dagger J_j^z-\gamma^* J_j^+)\right]\\&-\sum_{j=1}^{M}\frac{\partial}{\partial J_j^z}[-\gamma_{||}(J_j^z+N_j)-2g_j(J_j^+\alpha+J_j^-\alpha^\dagger)]+\gamma_p\sum_{j=1}^{M}\frac{\partial^2}{\partial J_j^-\partial J_j^+}(J_j^z+N_j)\\&\left.+\tfrac{1}{2}\sum_{j=1}^{M}\left[\frac{\partial^2}{\partial J_j^{-2}}(2g_j\alpha J_j^-)+\frac{\partial^2}{\partial J_j^{+2}}(2g_j\alpha^\dagger J_j^+)\right]+\tfrac{1}{2}\sum_{j=1}^{M}\frac{\partial^2}{\partial J_j^{z2}}[2\gamma_{||}(J_j^z+N_j)-4g_j(J_j^+\alpha+J_j^-\alpha^\dagger)]\right]P(\boldsymbol{\alpha},t)\\\equiv&\left[\frac{\partial}{\partial\alpha_\mu}A_\mu(\boldsymbol{\alpha})+\frac{1}{2}\frac{\partial}{\partial\alpha_\mu}\frac{\partial}{\partial\alpha_\nu}D_{\mu\nu}(\boldsymbol{\alpha})\right]P(\boldsymbol{\alpha},t) \ .\end{aligned} \tag{6}$$

Here $\mu,\nu=1,2,3,\ldots,3M+2$,

$$\alpha=(\alpha,\alpha^\dagger;J_1^-,\ldots,J_M^-;J_1^z,\ldots,J_M^z;J_1^+,\ldots,J_M^+)\ ,$$
$$\kappa'=\kappa(1+i\varphi),\quad \gamma=\gamma_\perp(1+i\delta)\ , \tag{7}$$
$$\varphi\equiv\frac{\omega_c-\omega_I}{\kappa},\quad \delta\equiv\frac{\omega_a-\omega_I}{\gamma_\perp}\ .$$

In the positive P representation each of the derivatives $\partial/\partial\alpha_\mu$ is interpreted either as $\partial/\partial\alpha_\mu^x$ or $-i(\partial/\partial\alpha_\mu^y)$, where $\alpha_\mu=\alpha_\mu^x+i\alpha_\mu^y$, so that Eq. (6) is a Fokker-Planck equation in $6M+4$ real dimensions with positive diffusion.[2,3] The Ito stochastic differential equations corresponding to this Fokker-Planck equation are[9,10]

$$\dot\alpha=-\kappa(1+i\varphi)\alpha+\sum_{j=1}^M g_jJ_j^-+\kappa\mathscr{E}\ ,$$
$$\dot\alpha^\dagger=-\kappa(1-i\varphi)\alpha^\dagger+\sum_{j=1}^M g_jJ_j^++\kappa\mathscr{E}^*\ ,$$
$$\dot J_j^-=g_j\alpha J_j^z-\gamma_\perp(1+i\delta)J_j^-+\Gamma_{J_j^-}\ , \tag{8}$$
$$\dot J_j^+=g_j\alpha^\dagger J_j^z-\gamma_\perp(1-i\delta)J_j^++\Gamma_{J_j^+}\ ,$$
$$\dot J_j^z=-\gamma_\parallel(J_j^z+N_j)-2g_j(\alpha J_j^++\alpha^\dagger J_j^-)+\Gamma_{J_j^z}\ ,$$
$$j=1,2,\ldots,M\ ,$$

where $\Gamma_{J_j^-}$, $\Gamma_{J_j^+}$, and $\Gamma_{J_j^z}$ are Gaussian distributed noises whose nonzero correlations are

$$\langle\Gamma_{J_i^z}(t)\Gamma_{J_j^z}(t')\rangle=[2\gamma_\parallel(J_j^z+N_j)-4g_j(J_j^+\alpha+J_j^-\alpha^\dagger)]\times\delta_{ij}\delta(t-t')\ ,$$
$$\langle\Gamma_{J_i^-}(t)\Gamma_{J_j^-}(t')\rangle=2g_j\alpha J_j^-\delta_{ij}\delta(t-t')\ ,$$
$$\langle\Gamma_{J_i^+}(t)\Gamma_{J_j^+}(t')\rangle=2g_j\alpha^\dagger J_j^+\delta_{ij}\delta(t-t')\ , \tag{9}$$
$$\langle\Gamma_{J_i^+}(t)\Gamma_{J_j^-}(t')\rangle=\langle\Gamma_{J_j^-}(t)\Gamma_{J_i^+}(t')\rangle=\gamma_p(J_j^z+N_j)\delta_{ij}\delta(t-t')\ .$$

In the good-cavity limit the atoms decay much faster than the cavity field ($\gamma_\perp,\gamma_\parallel\gg\kappa$) and therefore the atomic variables can be adiabatically eliminated. We set the derivatives $\partial J_j^\pm/\partial t,\partial J_j^z/\partial t$ equal to zero and solve for J_j^-, J_j^+, and J_j^z in terms of α and $\alpha^\dagger$, and $\Gamma_{J_j^-}$, $\Gamma_{J_j^+}$, and $\Gamma_{J_j^z}$. We substitute the solutions for J_j^- and J_j^+ into the field equations, including their dependence on $\Gamma_{J_j^-}$, $\Gamma_{J_j^+}$, and $\Gamma_{J_j^z}$. We evaluate the correlation functions in (9) by substituting the solutions for the atomic variables as functions of α and $\alpha^\dagger$ alone, dropping their dependence on $\Gamma_{J_j^-}$, $\Gamma_{J_j^+}$, and $\Gamma_{J_j^z}$. This approximate procedure is consistent with the linearization—valid in the small-noise limit—introduced further on. The equations for the field become

$$\dot{\bar x}=-(1+i\varphi)\bar x+y-\frac{2(1-i\delta)\bar x}{(1+\delta^2)}\sum_{j=1}^M\frac{C_j}{1+\frac{1}{1+\delta^2}\bar X_j}+\frac{1}{\sqrt{n_0}}\tilde\Gamma(\tau)\ ,$$
$$\dot{\bar x}^\dagger=-(1-i\varphi)\bar x^\dagger+y^*-\frac{2(1+i\delta)\bar x^\dagger}{(1+\delta^2)}\sum_{j=1}^M\frac{C_j}{1+\frac{1}{1+\delta^2}\bar X_j}+\frac{1}{\sqrt{n_0}}\tilde\Gamma^\dagger(\tau)\ , \tag{10}$$

where time is scaled in units of the cavity decay time, $\tau\equiv\kappa t$. The noise correlations are

$$\langle\tilde\Gamma(\tau)\tilde\Gamma(\tau')\rangle=-\left[\sum_{j=1}^M\frac{2C_j\bar x_j^2}{(1+\delta^2+\bar X_j)^3}[(1-i\delta)^3f+i\delta(1-f)(1-i\delta)\bar X_j+\tfrac{1}{2}\bar X_j^2]\right]\delta(\tau-\tau')$$
$$=-\left[\frac{2C\bar x^2V_{\rm eff}}{s^2}\sum_{j=1}^M\frac{|U(\mathbf{r}_j)|^4\Delta V_j}{\left[1+\delta^2+\frac{\bar XV_{\rm eff}}{s}|U(\mathbf{r}_j)|^2\right]^3}\times\left[(1-i\delta)^3f+i\delta(1-i\delta)(1-f)\frac{\bar XV_{\rm eff}}{s}|U(\mathbf{r}_j)|^2+\frac{1}{2}\frac{\bar X^2V_{\rm eff}^2}{s^2}|U(\mathbf{r}_j)|^4\right]\right]\delta(\tau-\tau')$$
$$\equiv-P\delta(\tau-\tau')\ ,$$

$$\langle \tilde{\Gamma}^{\dagger}(\tau)\tilde{\Gamma}^{\dagger}(\tau')\rangle = -\left[\sum_{j=1}^{M}\frac{2C_j\bar{x}_j^{\dagger 2}}{(1+\delta^2+\bar{X}_j)^3}[(1+i\delta)^3 f - i\delta(1-f)(1+i\delta)\bar{X}_j + \tfrac{1}{2}\bar{X}_j^{\,2}]\right]\delta(\tau-\tau')$$

$$= -\left[\frac{2C\bar{x}^{\dagger 2}V_{\rm eff}}{s^2}\sum_{j=1}^{M}\frac{|U(\mathbf{r}_j)|^4\Delta V_j}{\left[1+\delta^2+\dfrac{\bar{X}V_{\rm eff}}{s}|U(\mathbf{r}_j)|^2\right]^3} \times\left[(1+i\delta)^3 f - i\delta(1+i\delta)(1-f)\frac{\bar{X}V_{\rm eff}}{s}|U(\mathbf{r}_j)|^2 + \frac{1}{2}\frac{\bar{X}^2V_{\rm eff}^2}{s^2}|U(\mathbf{r}_j)|^4\right]\right]\delta(\tau-\tau')$$

$$\equiv -P^{\dagger}\delta(\tau-\tau') , \tag{11}$$

$$\langle \tilde{\Gamma}(\tau)\tilde{\Gamma}^{\dagger}(\tau')\rangle = \langle \tilde{\Gamma}^{\dagger}(\tau)\tilde{\Gamma}(\tau')\rangle$$

$$= \left[\sum_{j=1}^{M}\frac{2C_j\bar{X}_j}{(1+\delta^2+\bar{X}_j)^3}\{(1+\delta^2)(1-f)+[2+(1-f)\delta^2]\bar{X}_j + \tfrac{1}{2}\bar{X}_j^{\,2}\}\right]\delta(\tau-\tau')$$

$$= \left[\frac{2C\bar{X}V_{\rm eff}}{s^2}\sum_{j=1}^{M}\frac{|U(\mathbf{r}_j)|^4\Delta V_j}{\left[1+\delta^2+\dfrac{\bar{X}V_{\rm eff}}{s}|U(\mathbf{r}_j)|^2\right]^3} \times\left[(1+\delta^2)(1-f)+[2+(1-f)\delta^2]\frac{\bar{X}V_{\rm eff}}{s}|U(\mathbf{r}_j)|^2 + \frac{1}{2}\frac{\bar{X}^2V_{\rm eff}^2}{s^2}|U(\mathbf{r}_j)|^4\right]\right]\delta(\tau-\tau')$$

$$\equiv Q\delta(\tau-\tau') .$$

Here,

$$\bar{x}_j \equiv \frac{\alpha}{\sqrt{n_{0j}}},\quad \bar{x}_j^{\dagger} \equiv \frac{\alpha^{\dagger}}{\sqrt{n_{0j}}},\quad \bar{X}_j \equiv \bar{x}_j\bar{x}_j^{\dagger} ,$$

$$C_j = \frac{g_j^2 N_j}{2\gamma_{\perp}\kappa} = \frac{g_0^2\rho|U(\mathbf{r}_j)|^2\Delta V_j}{2\gamma_{\perp}\kappa} = \frac{C|U(\mathbf{r}_j)|^2\Delta V_j}{s} ,$$

$$n_{0j} \equiv \frac{\gamma_{\perp}\gamma_{\parallel}}{4g_j^2} = \frac{sn_0}{V_{\rm eff}|U(\mathbf{r}_j)|^2} ,$$

$$C \equiv \frac{g_0^2\rho s}{2\gamma_{\perp}\kappa},\quad n_0 \equiv \frac{\gamma_{\perp}\gamma_{\parallel}V_{\rm eff}}{4g_0^2 s} , \tag{12}$$

$$y \equiv \mathscr{E}/\sqrt{n_0},\quad \bar{x} \equiv \alpha/\sqrt{n_0},\quad \bar{x}^{\dagger} \equiv \alpha^{\dagger}/\sqrt{n_0} ,$$

$$Y \equiv yy^{*},\quad \bar{X} \equiv \bar{x}\bar{x}^{\dagger} ,$$

$$f \equiv \frac{\gamma_{\parallel}}{2\gamma_{\perp}},\quad s \equiv \frac{l}{L} .$$

$V_{\rm eff}$ is the effective mode volume for the cavity of length L and is given by

$$V_{\rm eff} = \frac{s^2}{\int\int\int_{\bar{V}}|U(\mathbf{r})|^4 d^3r} . \tag{13}$$

$\bar{V}$ is the sample volume, ρ is the density of the uniformly distributed atomic sample of length l, and ΔV_j is the volume of the jth section ($N_j=\rho\Delta V_j$). $U(\mathbf{r})$ is the normalized field mode function.

The steady-state solutions to Eq. (10) satisfy the state equation

$$Y = X\left|(1+i\varphi)+\frac{2(1-i\delta)}{1+\delta^2}\sum_{j=1}^{M}\frac{C_j}{1+X_j/(1+\delta^2)}\right|^2 , \tag{14}$$

where we write steady-state field variables without the overbar. A given mode function $U(\mathbf{r}_j)$ allows one to carry out the summation explicitly, as we will see in Secs. III and IV.

Comparing Eqs. (10) and (11) with the corresponding results in OBII [Eqs. (21), (23), and (24)], we see that a simple prescription can be applied at the level of the Fokker-Planck equation or of the stochastic differential equations to obtain our expressions from those in OBII. If we view the results of OBII as applicable to one of the N_j small regions, and if we sum over all regions to obtain the total drift and diffusion matrices (that is, the total source field in the field evolution equation), then we reproduce the results of the current treatment. This ana-

lytic calculation is possible for a spatially varying field mode when we employ the statistical limit discussed above together with the good-cavity limit. We stress that this procedure is applicable only at the level of the Fokker-Planck or stochastic differential equations. The formulas quoted in OBII for quantities such as the spectral density cannot be simply averaged to extend them to the case of a nonuniform field mode.

Since a complete solution to the nonlinear stochastic equations (10) (or equivalently to the associated nonlinear Fokker-Planck equation) is not in general possible, we address the question of the field fluctuations by linearizing about the steady state. We linearize about solutions to Eq. (14) with $x^{\dagger}=x^{*}$, corresponding to steady-state solutions of the semiclassical theory ($\bar{x}$ and $\bar{x}^{\dagger}$ are not necessarily complex conjugate in the positive P representation). After carrying out the summations in Eq. (10), we introduce the small deviations $(\delta\bar{x},\delta\bar{x}^{\dagger})=(\bar{x}-x,\bar{x}^{\dagger}-x^{*})$ and evaluate the nonlinear noise sources with the steady-state values x and x^{*}. The general form of the resulting linearized equations is

$$\begin{bmatrix} \delta\dot{\bar{x}} \\ \delta\dot{\bar{x}}^{\dagger} \end{bmatrix} = -M_{\mathrm{SS}} \begin{bmatrix} \delta\bar{x} \\ \delta\bar{x}^{\dagger} \end{bmatrix} + \frac{1}{\sqrt{n_0}} B \begin{bmatrix} \xi_1(\tau) \\ \xi_2(\tau) \end{bmatrix} , \tag{15}$$

where $\langle \xi_i(\tau)\xi_j(\tau')\rangle = \delta(\tau-\tau')\delta_{ij}$, $i,j=1,2$, $B^{T}B=D_{\mathrm{SS}}$, and

$$M_{\mathrm{SS}} \equiv \begin{bmatrix} a & b \\ b^{*} & a^{*} \end{bmatrix}, \quad D_{\mathrm{SS}} \equiv \begin{bmatrix} -P_{\mathrm{SS}} & Q_{\mathrm{SS}} \\ Q_{\mathrm{SS}} & -P_{\mathrm{SS}}^{*} \end{bmatrix} \tag{16}$$

with P and Q defined in (11), and evaluated at steady state ($\bar{x}=x$, $\bar{x}^{\dagger}=x^{*}$) and a and b given by linearizing (10) as

$$\begin{aligned} a &\equiv (1+i\varphi) + \frac{2(1-i\delta)C}{s} \sum_{j=1}^{M} \frac{|U(\mathbf{r}_j)|^2 \Delta V_j}{1+\delta^2+\frac{V_{\mathrm{eff}}X}{s}|U(\mathbf{r}_j)|^2} - \frac{2(1-i\delta)XCV_{\mathrm{eff}}}{s^2} \sum_{j=1}^{M} \frac{|U(\mathbf{r}_j)|^4 \Delta V_j}{\left[1+\delta^2+\frac{V_{\mathrm{eff}}X}{s}|U(\mathbf{r}_j)|^2\right]^2} , \\ b &\equiv -\frac{2(1-i\delta)x^2CV_{\mathrm{eff}}}{s^2} \sum_{j=1}^{M} \frac{|U(\mathbf{r}_j)|^4 \Delta V_j}{\left[1+\delta^2+\frac{V_{\mathrm{eff}}X}{s}|U(\mathbf{r}_j)|^2\right]^2} . \end{aligned} \tag{17}$$

The steady-state covariance matrix C_{SS} can be written in terms of the linearized drift and diffusion coefficients a, b, P_{SS}, and Q_{SS} by solving the matrix equation[11]

$$M_{\mathrm{SS}}C_{\mathrm{SS}} + C_{\mathrm{SS}}M_{\mathrm{SS}}^{T} = \frac{1}{n_0} D_{\mathrm{SS}} , \tag{18}$$

where

$$C_{\mathrm{SS}} \equiv \begin{bmatrix} \langle \delta\bar{x}\delta\bar{x}\rangle_{\mathrm{SS}} & \langle \delta\bar{x}\delta\bar{x}^{\dagger}\rangle_{\mathrm{SS}} \\ \langle \delta\bar{x}^{\dagger}\delta\bar{x}\rangle_{\mathrm{SS}} & \langle \delta\bar{x}^{\dagger}\delta\bar{x}^{\dagger}\rangle_{\mathrm{SS}} \end{bmatrix} \equiv \begin{bmatrix} C_{11} & C_{12} \\ C_{21} & C_{22} \end{bmatrix} . \tag{19}$$

From C_{SS} we are able to obtain the ratio of incoherent intensity to coherent intensity ($\delta I_{\mathrm{inc}}/I_{\mathrm{coh}}$) and the intensity correlation function of the intracavity field $[g^{(2)}(0)-1]$ as follows:

$$\frac{\delta I_{\mathrm{inc}}}{I_{\mathrm{coh}}} \equiv \frac{\langle \delta\bar{x}^{\dagger}\delta\bar{x}\rangle_{\mathrm{SS}}}{X} = \frac{Q_{\mathrm{SS}}|a|^2 + \mathrm{Re}(abP_{\mathrm{SS}}^{*})}{2n_0X\,\mathrm{Re}(a)(|a|^2-|b|^2)} , \tag{20}$$

$$\begin{aligned} g^{(2)}(0)-1 &\equiv \frac{\langle \bar{x}^{\dagger 2}\bar{x}^{2}\rangle - \langle \bar{x}^{\dagger}\bar{x}\rangle^2}{\langle \bar{x}^{\dagger}\bar{x}\rangle^2} \\ &= \Bigg\{ [Q_{\mathrm{SS}}|a|^2 + \mathrm{Re}(abP_{\mathrm{SS}}^{*})] \\ &\quad - \left[\mathrm{Re}(a)(|a|^2-|b|^2)\,\mathrm{Re}\left(\frac{xaP_{\mathrm{SS}}^{*}}{x^{*}}\right) \right. \\ &\quad \left. + \mathrm{Re}\left(\frac{xab^{*}}{x^{*}}\right)[Q_{\mathrm{SS}}|a|^2 + \mathrm{Re}(abP_{\mathrm{SS}}^{*})] \right] \Big/ |a|^2 \Bigg\} \Big/ [n_0X\,\mathrm{Re}(a)(|a|^2-|b|^2)] . \end{aligned} \tag{21}$$

In Secs. III and IV we present two examples to demonstrate explicitly how the linearized coefficients (a,b,P_{SS},Q_{SS}) are calculated and how the standard results of the plane-wave ring interferometer are modified. While the discussion is restricted to the quantities $\delta I_{inc}/I_{coh}$ and $g^{(2)}(0)-1$, our formalism can as well be applied to address other questions such as photon antibunching $g^{(2)}(\tau)-1$ and squeezed state production in a spatially varying field mode. The issue of squeezing will be covered in a separate publication.[12]

To close this section on the general development of the theory, we note that one particular feature that emerges from our analysis is that there exist quite generally unified limits in which the quantum statistical features become independent of the spatial structure of the cavity mode. In either the weak field limit $X\to 0$ or the dispersive limit $X/(1+\delta^2)\to 0$, it is easy to see that at steady state Eqs. (11) and (17) become

$$\langle \tilde{\Gamma}(\tau)\tilde{\Gamma}(\tau')\rangle \approx -\left[\frac{2Cx^2(1-i\delta)^3 f}{s^2(1+\delta^2)^3}\left[V_{\text{eff}}\sum_{j=1}^{M}|U(\mathbf{r}_j)|^4\Delta V_j\right]\right]\delta(\tau-\tau')\ ,$$

$$\langle \tilde{\Gamma}^\dagger(\tau)\tilde{\Gamma}(\tau')\rangle = \langle \tilde{\Gamma}(\tau)\tilde{\Gamma}^\dagger(\tau')\rangle \approx \left[\frac{2CX(1-f)}{s^2(1+\delta^2)^2}\left[V_{\text{eff}}\sum_{j=1}^{M}|U(\mathbf{r}_j)|^4\Delta V_j\right]\right]\delta(\tau-\tau')\ , \tag{22}$$

$$\langle \tilde{\Gamma}^\dagger(\tau)\tilde{\Gamma}^\dagger(\tau')\rangle \approx -\left[\frac{2Cx^{*2}(1+i\delta)^3 f}{s^2(1+\delta^2)^3}\left[V_{\text{eff}}\sum_{j=1}^{M}|U(\mathbf{r}_j)|^4\Delta V_j\right]\right]\delta(\tau-\tau')\ ,$$

$$a\approx(1+i\varphi)+\frac{2(1-i\delta)C}{s(1+\delta^2)}\left[\sum_{j=1}^{M}|U(\mathbf{r}_j)|^2\Delta V_j\right]-\frac{2CX(1-i\delta)}{s^2(1+\delta^2)^2}\left[V_{\text{eff}}\sum_{j=1}^{M}|U(\mathbf{r}_j)|^4\Delta V_j\right], \tag{23}$$

$$b\approx-\frac{2Cx^2(1-i\delta)}{s^2(1+\delta^2)^2}\left[V_{\text{eff}}\sum_{j=1}^{M}|U(\mathbf{r}_j)|^4\Delta V_j\right]. \tag{24}$$

From Eq. (13) and the definition of $U(\mathbf{r}_j)$ as a normalized mode function, we have

$$\lim_{\substack{M\to\infty\\ \Delta V_j\to 0}}\sum_{j=1}^{M}|U(\mathbf{r}_j)|^4\Delta V_j=\int\int\int_{\bar{V}}|U(\mathbf{r})|^4 d^3r=\frac{s^2}{V_{\text{eff}}}\ , \tag{25}$$

$$\lim_{\substack{M\to\infty\\ \Delta V_j\to 0}}\sum_{j=1}^{M}|U(\mathbf{r}_j)|^2\Delta V_j=\int\int\int_{\bar{V}}|U(\mathbf{r})|^2 d^3r=s\ . \tag{26}$$

Equations (22)–(26) mean that the linearized coefficients a, b, P_{SS}, and Q_{SS} and hence the quantum statistical features are independent of the spatial configuration of the cavity mode in the limit of a weak intracavity field or for detuning δ large enough to be in the dispersive region.[5]

III. SINGLE GAUSSIAN MODE FIELD INSIDE A RING CAVITY

One important example of a nonuniform field is a Gaussian profile in a ring cavity.[13] We will discuss this example first. Following the discussion of Sec. II, we divide the Gaussian field mode into M cylindrical shells along the cavity axis, each with radius r_j and thickness Δr_j, and each containing N_j atoms. For simplicity we will neglect the z dependence of the beam waist W, which is reasonable for a sample of length l much less than the Rayleigh length.[14] The normalized mode function for the Gaussian-beam ring cavity in this approximation is

$$U(\mathbf{r}_j)=\left[\frac{2}{\pi LW^2}\right]^{1/2}e^{-r_j^2/W^2}\ , \tag{27}$$

where L is the cavity length and η is set to zero. The normalization is chosen such that

$$\int\int\int_V dV\,|U(\mathbf{r})|^2=1 \tag{28}$$

with the radial integral extending to infinity and the longitudinal integral extending over the cavity length. Then, from Eq. (13)

$$V_{\text{eff}}=(\pi W^2 L)s\ . \tag{29}$$

By taking the continuum limit, $M\to\infty$, $\Delta r_j\to 0$, for all shells, we can convert the summations appearing in Sec. II into integrations, as, for example,

$$\lim_{\substack{M\to\infty\\ \Delta r_j\to 0}}\sum_{j=1}^{M}\frac{C_j}{1+\frac{1}{1+\delta^2}X_j}=\frac{2C}{(\pi W^2L)s}\int\int\int_{\bar{V}}\frac{d^3r\,e^{-2r^2/W^2}}{1+\frac{2X}{1+\delta^2}e^{-2r^2/W^2}}$$

$$=\frac{C(1+\delta^2)}{2X}\ln\left[1+\frac{2X}{1+\delta^2}\right]. \tag{30}$$

Combining Eqs. (30) and (14), we obtain the standard state equation in agreement with Refs. 5, 14, and 15, namely,

$$Y=X\left|(1+i\varphi)+\frac{C(1-i\delta)}{X}\ln\left[1+\frac{2X}{1+\delta^2}\right]\right|^2. \tag{31}$$

The linearized drift coefficients a and b can be obtained from (17) using the integration of (30) as

$$\lim_{\substack{M\to\infty\\ \Delta r_j\to 0}} a=(1+i\varphi)+\frac{2C(1-i\delta)}{1+\delta^2+2X}\ ,$$
$$\lim_{\substack{M\to\infty\\ \Delta r_j\to 0}} b=\frac{(1-i\delta)Cx^2}{X}\left[\frac{2}{1+\delta^2+2X}-\frac{1}{X}\ln\left[1+\frac{2X}{1+\delta^2}\right]\right]. \tag{32}$$

The diffusion coefficients are calculated from (11) in the same way, leading to

$$\lim_{\substack{M\to\infty\\ \Delta r_j\to 0}} P_{SS}=\frac{8Cx^2}{(\pi W^2L)s}\int\int\int_{-\infty}^{\infty} d^3r\frac{e^{-4r^2/W^2}}{(1+\delta^2+2Xe^{-2r^2/W^2})^3}$$
$$\times[(1-i\delta)^3f+2i\delta(1-f)(1-i\delta)Xe^{-2r^2/W^2}+2X^2e^{-4r^2/W^2}]$$
$$=Cx^2\left[\frac{1}{(1+\delta^2+2X)^2}\left[\frac{2(1-i\delta)^3f}{1+\delta^2}+4X+3[\delta^2(1+2f)-2i\delta(1-f)+3]\right.\right.$$
$$\left.\left.+\frac{1+\delta^2}{X}[(1+2f)\delta^2-2i\delta(1-f)+3]\right]-\frac{(1+2f)\delta^2-2i\delta(1-f)+3}{2X^2}\ln\left[1+\frac{2X}{1+\delta^2}\right]\right] \tag{33}$$

and

$$\lim_{\substack{M\to\infty\\ \Delta r_j\to 0}} Q_{SS}=\frac{8C}{(\pi W^2L)s}\int\int\int_{-\infty}^{\infty} d^3r\frac{e^{-4r^2/W^2}}{(1+\delta^2+2Xe^{-2r^2/W^2})^3}$$
$$\times\{(1+\delta^2)(1-f)+2[2+(1-f)\delta^2]Xe^{-2r^2/W^2}+2X^2e^{-4r^2/W^2}\}$$
$$=C\left[\frac{4X^2-(1+2f)(1-3\delta^2)X-(1+\delta^2)[1-\delta^2(1+2f)]}{(1+\delta^2+2X)^2}+\frac{1-\delta^2(1+2f)}{2X}\ln\left[1+\frac{2X}{1+\delta^2}\right]\right]. \tag{34}$$

Substituting (32)—(34) into (20) and (21), we obtain explicit expressions for $\delta I_{\rm inc}/I_{\rm coh}$ and $g^{(2)}(0)-1$.

In order to illustrate the effects due to the Gaussian profile, we plot in Figs. 1—3 results for the Gaussian-beam traveling-wave cavity, together with those from the plane-wave theory for a ring cavity from OBII and Ref. 16. From Figs. 1 and 2 we see that for weak fields the feature of sub-Poissonian photon statistics $[g^{(2)}(0)-1<0]$ is preserved in the case of the Gaussian beam. The nonuniform transverse profile does, however, tend to reduce the degree of nonclassical behavior, since for equal values of X the Gaussian profile contains a range of intensities X_j higher than that of the corresponding plane wave $[X_j=2X\exp(-2r_j^2/W^2)]$. $g^{(2)}(0)<1$ is a weak field effect in this system. As X increases towards turning point, the behavior of $g^{(2)}(0)$ is dominated by the deterministic divergence of the field fluctuations. Figures 1(a) and 2 show $[g^{(2)}(0)-1]$ for equal values of X in the plane-wave ring and Gaussian ring theories for several cavity detunings. On the other hand, Fig. 1(b) displays $[g^{(2)}(0)-1]$ versus an intensity $\tilde{X}=X/X_1$, with X_1 the intensity in either theory at the turning point on the lower branch (for the plane wave, $X_1=1.05$; for the Gaussian ring, $X_1'=2.19$). Since $X_1'>X_1$, the nonclassical behavior is seen to vanish more quickly for the Gaussian beam when a normalization in terms of a "critical parameter" is employed.

Figure 3 compares the dependence of the ratio of incoherent to coherent intensities on normalized intensity X/X_0 for the plane-wave and Gaussian rings. We have chosen to make the comparison at the critical point in each case, with X_0 as the corresponding critical intensity. Apart from the divergence near the critical point (where the two theories should asymptotically merge), we see that in general the incoherent intensities are larger for the Gaussian beam below the critical point. This behavior is again associated with the larger values of intracavity field for a given X or X/X_0 in the Gaussian ring. Above the critical point the ratio $R=n_0\delta I/I$ tends to be smaller in the Gaussian-beam case since the actual intensities X_j involved tend to drive the incoherent processes to saturation more quickly than in the plane-wave case. Figure 3(d) seems to be an exception to this state of affairs for $X/X_0>1$ where the ratio R is smaller for the plane-wave ring. This behavior is due in large measure to the very different onset of divergence of the deterministic eigenvalues in the two cases. For $X/X_0\geq 6.5$, the curves in Fig. 3(d) cross with the result that the ratio R is smaller for the Gaussian beam for large X/X_0 as in Figures 3(a)—3(c).

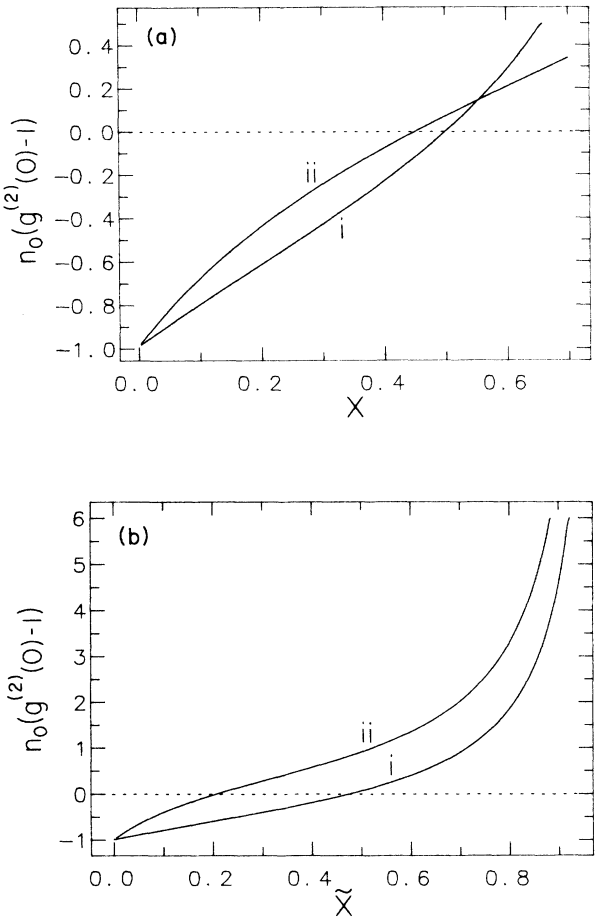

FIG. 1. Normalized intensity variance $n_0[g^{(2)}(0)-1]$ vs intracavity intensity. Curve i in each case is for the plane-wave ring cavity, while ii is for the Gaussian-beam ring [Eq. (27)]. Atomic detuning $\delta=0$, cavity detuning $\varphi=0$, with $f=1$ and $C=40$. (a) Abscissa is actual intracavity intensity X [Eq. (12)]; (b) abscissa is normalized variable $\tilde{X}=X/X_1$ with X_1 the intensity at the lower turning point [X_1 (plane-wave ring)$=1.05$; X_1 (Gaussian-beam ring)$=2.19$]. Note that $g^{(2)}(0)<1$ corresponds to the nonclassical effect of sub-Poissonian photon statistics.

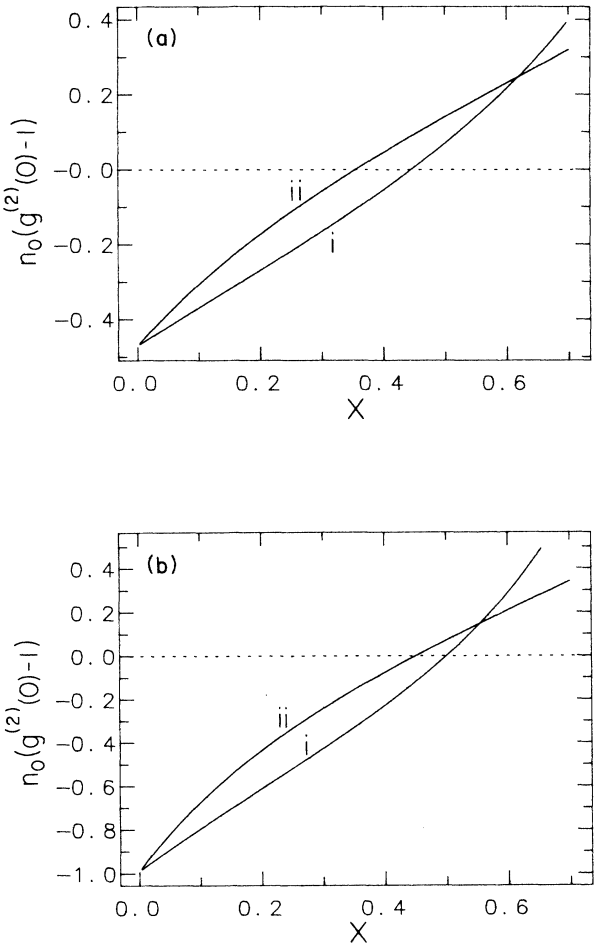

FIG. 2. $n_0[g^{(2)}(0)-1]$ vs intracavity intensity X. Curve i is for plane-wave ring cavity; curve ii is for Gaussian-beam ring. (a) $\delta=0.5$, $\varphi=0.0$, $f=1$, $C=40$; (b) $\delta=0.0$, $\varphi=0.5$, $f=1$, $C=40$.

IV. PLANE-WAVE FABRY-PEROT INTERFEROMETER

Another interesting and important example related to current experiments is a standing-wave cavity.[17] For the purpose of illustrating our method, we present the case of a plane-wave rather than of a Gaussian mode in the standing-wave interferometer. The latter case can be treated with our formalism; however, we wish to examine separately contributions due to the standing-wave structure and due to the Gaussian transverse profile.

Due to the symmetry of this problem, we can divide our sample into sections of length $\lambda/4$, each of which makes an identical contribution. For a sample length $l \gg \lambda$, we set $n\lambda=l$ with n an integer and divide each $\lambda/4$ region into M small slices over which the field can be considered as constant. The summation over all N atoms is then expressed as

$$\sum_{j=1}^{N} = 4n \sum_{j=1}^{M} \sum_{i=1}^{N_j} \tag{35}$$

with N_j atoms in the jth section. We will write

$$\Delta V_j = \Delta z_j A \tag{36}$$

with z_j as the longitudinal dimension along the cavity length and A as the cross-sectional area of the cavity. By requiring $\int\int\int_V dV\,|U(\mathbf{r}_j)|^2=1$, we find for the normalized mode function in the standing-wave cavity (with $\eta=0$),

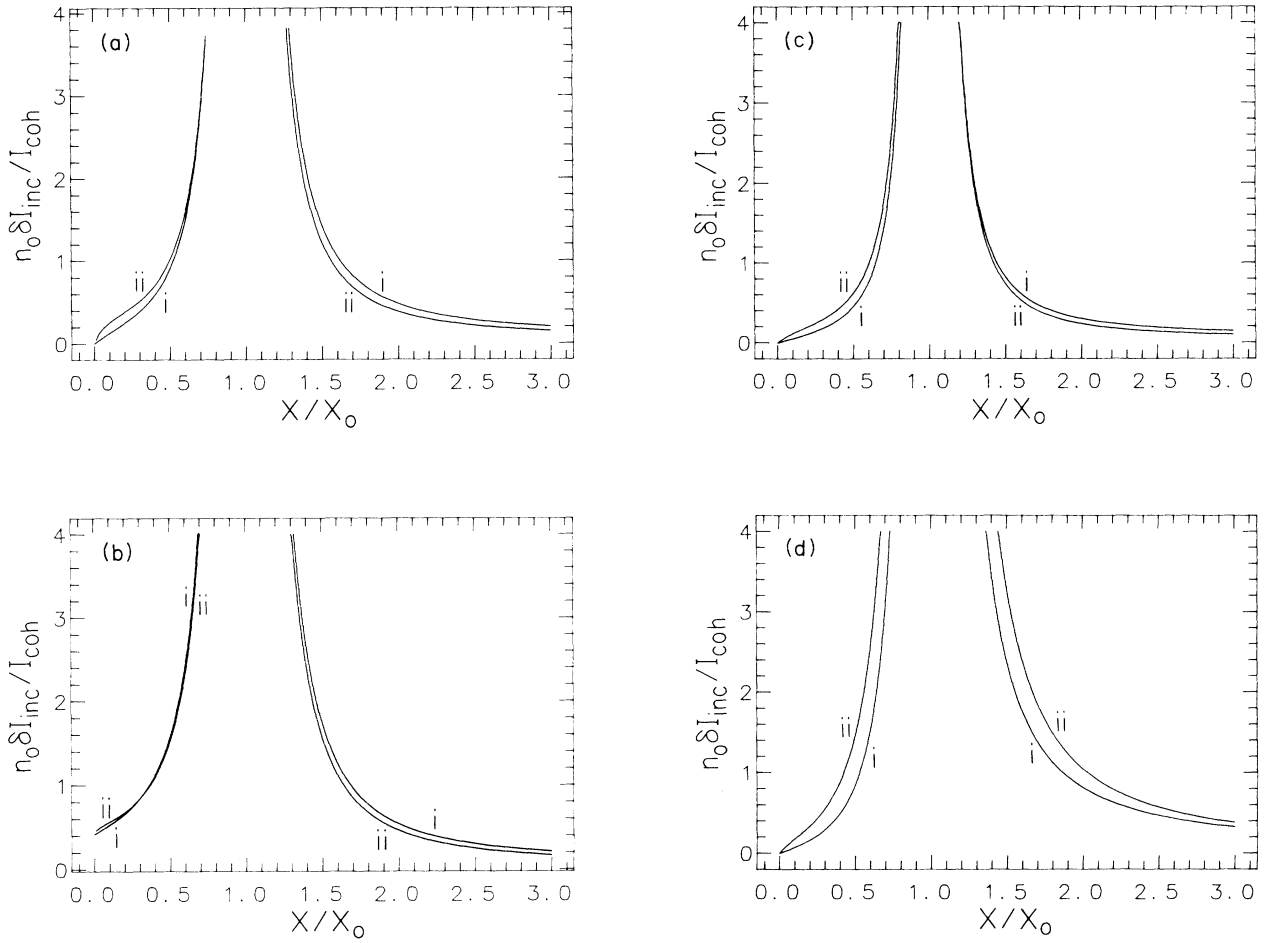

FIG. 3. Ratio R of incoherent to coherent intensity $n_0\delta I_{\rm inc}/I_{\rm coh}$ vs X/X_0 with X_0 equal to critical intracavity intensity and C set to its critical value C_0. Curve i in each case is for the plane-wave ring cavity, while ii is for the Gaussian-beam ring. (a) $\delta=0$, $\varphi=0$, $f=1$; i, $X_0=3.00$, $C_0=4.00$; ii, $X_0=6.65$, $C_0=8.31$. (b) $\delta=0$, $\varphi=0$, $f=0.05$; i, $X_0=3.00$, $C_0=4.00$; ii, $X_0=6.65$, $C_0=8.31$. (c) $\delta=1$, $\varphi=1$, $f=1$; i, $X_0=4.00$, $C_0=5.20$; ii, $X_0=8.20$, $C_0=8.33$. (d) $\delta=1$, $\varphi=-1$, $f=1$; i, $X_0=6.00$, $C_0=8.00$; ii, $X_0=13.3$, $C_0=16.6$.

$$U(\mathbf{r}_j)=\left[\frac{2}{AL}\right]^{1/2}\cos(kz_j)\ , \tag{37}$$

and from Eq. (13),

$$V_{\rm eff}=(\tfrac{2}{3}AL)s\ . \tag{38}$$

By taking the continuum limit $M\to\infty$, $\Delta z_j\to 0$ for all j, the summation in (10) becomes

$$\lim_{\substack{M\to\infty\\ \Delta z_j\to 0}} 4n\sum_{j=1}^{M}\frac{C_j}{1+X_j/(1+\delta^2)} =\frac{3C(1+\delta^2)}{2X}\left[1-\frac{1}{[1+4X/3(1+\delta^2)]^{1/2}}\right]. \tag{39}$$

Equations (14) and (39) lead to the well-known state equation for the plane-wave Fabry-Perot cavity, namely,[5]

$$Y=X\left|(1+i\varphi)+(1-i\delta)\frac{3C}{X}\left[1-\frac{1}{[1+4X/3(1+\delta^2)]^{1/2}}\right]\right|^2. \tag{40}$$

As before, by using Eqs. (11) and (17), and performing the integrations, we obtain the drift and diffusion coefficients as follows:

$$\lim_{\substack{M\to\infty\\ \Delta z_j\to 0}} a=(1+i\varphi)+\frac{2C(1-i\delta)}{(1+\delta^2)[1+4X/3(1+\delta^2)]^{3/2}}\ , \tag{41}$$

$$\lim_{\substack{M\to\infty\\ \Delta z_j\to 0}} b=\frac{(1-i\delta)3C}{x^{*2}} \times\left[\frac{2X+1+\delta^2}{(1+\delta^2)[1+4X/3(1+\delta^2)]^{3/2}}-1\right],$$

$$\lim_{\substack{M\to\infty \\ \Delta z_j\to 0}} P_{\rm SS}=\frac{64nCx^2}{3Ls}\int_0^{\lambda/4}\frac{dz\cos^4(kz)}{[1+\delta^2+\frac{4}{3}X\cos^2(kz)]^3}[(1-i\delta)^3 f+i\delta(1-f)(1-i\delta)\tfrac{4}{3}X\cos^2(kz)+\tfrac{8}{9}X^2\cos^4(kz)]$$

$$=Cx^2\left[\frac{(1+2f)-\delta^2[4f+\delta^2(1-2f)]-i\delta[4f(1-\delta^2)+2(1+\delta^2)]}{(1+\delta^2)^3[1+4X/3(1+\delta^2)]^{5/2}}+\frac{1}{X}+\frac{2[1+f\delta^2-i\delta(1-f)]}{X(1+\delta^2)[1+4X/3(1+\delta^2)]^{3/2}}\right.$$

$$\left.-\frac{3}{X^2}\left[1-\frac{1}{[1+4X/3(1+\delta^2)]^{1/2}}\right]\left[\frac{3}{2}+\frac{\delta^2}{2}(1+2f)-i\delta(1-f)\right]\right], \tag{42}$$

and

$$\lim_{\substack{M\to\infty \\ \Delta z_j\to 0}} Q_{\rm SS}=C\left[1-\frac{X}{(1+\delta^2)^2[1+4X/3(1+\delta^2)]^{5/2}}[(1+2f)+\delta^2(1-2f)]\right.$$

$$\left.-\frac{2(1-f\delta^2)}{(1+\delta^2)[1+4X/3(1+\delta^2)]^{3/2}}+\frac{3}{X}\left[1-\frac{1}{[1+4X/3(1+\delta^2)]^{1/2}}\right]\left[\frac{1}{2}-\frac{\delta^2}{2}(1+2f)\right]\right]. \tag{43}$$

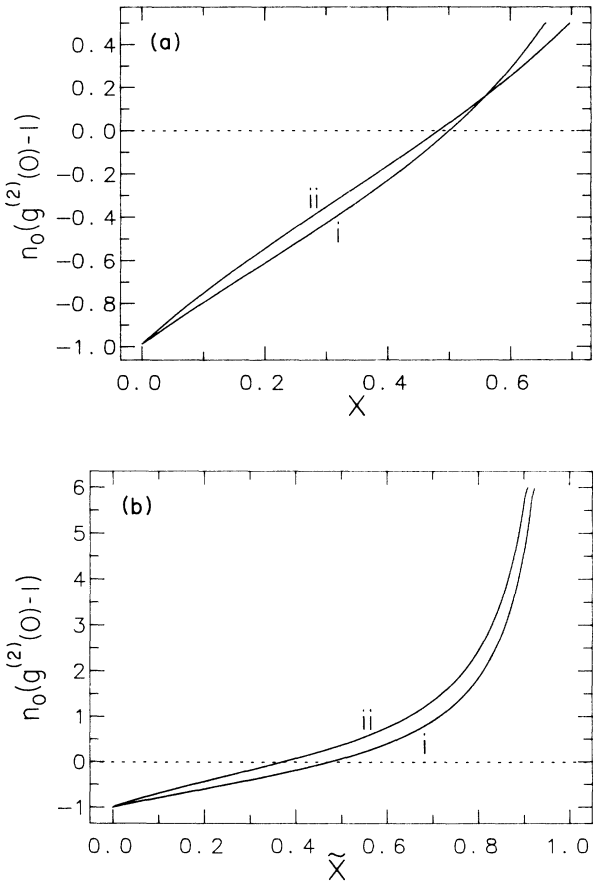

FIG. 4. $n_0[g^{(2)}(0)-1]$ vs intracavity intensity. Curve i in each case is for the plane-wave ring cavity, while ii is for the standing-wave cavity [Eq. (37)]. $\delta=0$, $\varphi=0$, $f=1$, $C=40$. (a) Abscissa is intracavity intensity X; (b) abscissa is normalized variable $\tilde{X}=X/X_1$ with X_1 the intensity at the lower turning point [X_1 (plane-wave ring)$=1.05$; X_1 (standing-wave cavity)$=1.29$].

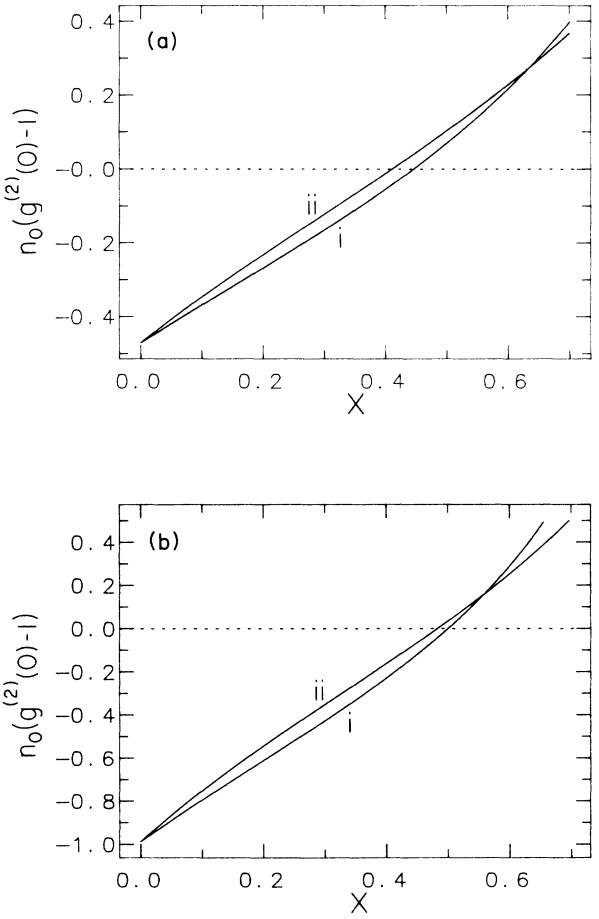

FIG. 5. $n_0[g^{(2)}(0)-1]$ vs intracavity intensity X. Curve i is for the plane-wave ring cavity; curve ii for standing-wave cavity. (a) $\delta=0.5$, $\varphi=0.0$, $f=1$, $C=40$; (b) $\delta=0.0$, $\varphi=0.5$, $f=1$, $C=40$.

Substituting (41)—(43) into (20) and (21) leads to explicit expressions for $\delta I_{\rm inc}/I_{\rm coh}$ and $g^{(2)}(0)-1$.

In Figs. (4)—(6) we compare these results for the plane-wave Fabry-Perot to those for the plane-wave ring cavity from OBII. From Figs. 4 and 5 we see that in qualitative terms the nonclassical behavior $g^{(2)}(0)<1$ is once again preserved in spite of the longitudinal standing-wave structure. The general reduction of this nonclassical effect relative to the plane-wave ring cavity is associated with values of the intracavity field $X_j=\frac{4}{3}X\cos^2(kz_j)$ larger than those for the plane-wave ring. Figure 6 gives plots of the ratio of incoherent to coherent intensities for the plane-wave ring and standing-wave cavities with the same qualitative features appearing as in Fig. 3. Indeed, the whole of the discussion relative to Figs. 1—3 for the Gaussian mode function in a ring cavity is applicable to the standing-wave case, with the exception that the longitudinal standing-wave profile results in much smaller deviations from the plane-wave theory. For example, the degradation in nonclassical features expressed by $g^{(2)}(0)$ is less severe in the standing-wave cavity than in the Gaussian ring. Further, the plane-wave ring and standing-wave cavity are remarkably similar in their predictions of $n_0\delta I_{\rm inc}/I_{\rm coh}$ versus X/X_0.

V. SUMMARY

We have presented an analysis of the quantum fluctuations for a collection of two-level atoms interacting with a spatially varying field mode of a high-finesse interferometer. The treatment is carried out in the limit in which the atomic variables relax on a time scale much shorter than that of the intracavity field. For this case we are able to obtain analytic expressions for the linearized field fluctuations. In particular, we have quoted results for the ratio

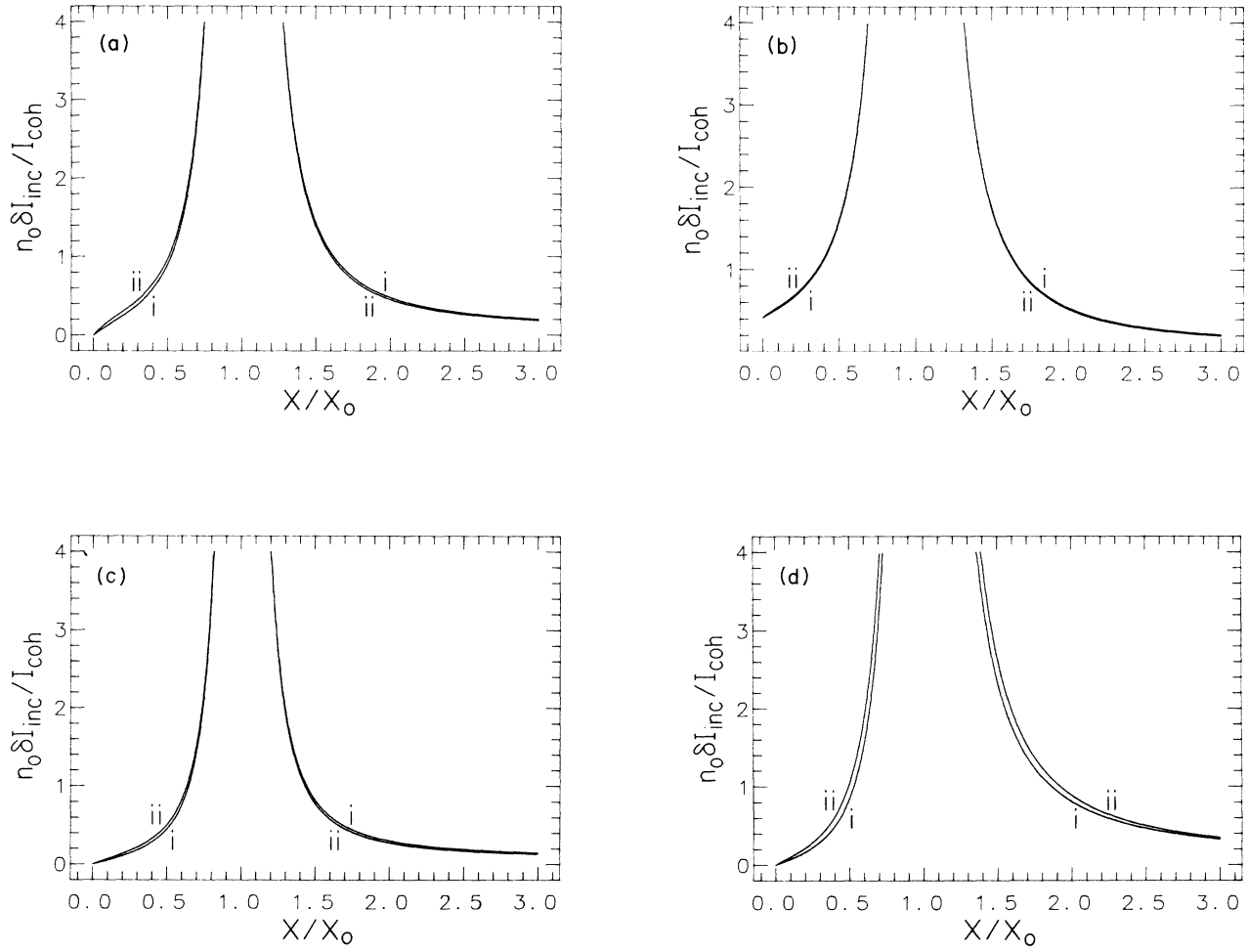

FIG. 6. Ratio R of incoherent to coherent intensity $n_0\delta_{\rm inc}/I_{\rm coh}$ vs X/X_0 with X_0 equal to critical intracavity intensity and C set to its critical value C_0. Curve i in each case is for the plane-wave ring cavity, while ii is for the standing-wave cavity. (a) $\delta=0$, $\varphi=0$, $f=1$; i, $X_0=3.00$, $C_0=4.00$; ii, $X_0=3.80$, $C_0=4.97$. (b) $\delta=0$, $\varphi=0$, $f=0.05$; i, $X_0=3.00$, $C_0=4.00$; ii, $X_0=3.80$, $C_0=4.97$. (c) $\delta=1$, $\varphi=1$, $f=1$; i, $X_0=4.00$, $C_0=5.20$; ii, $X_0=4.93$, $C_0=5.97$. (d) $\delta=1$, $\varphi=-1$, $f=1$; i, $X_0=6.00$, $C_0=8.00$; ii, $X_0=7.61$, $C_0=9.94$.

of incoherent to coherent intensity of the intracavity field and for the fourth-order field correlation function that describes intensity fluctuations of the intracavity field and sub-Poissonian photon statistics. Two examples of a Gaussian-mode traveling-wave cavity and a plane-wave Fabry-Perot have been examined in detail to illustrate the general theory and to provide a comparison with previous work on the plane-wave ring cavity. Not surprisingly, the general phenomenology is preserved in qualitative terms, but there are important quantitative modifications worth noting, especially with regard to possible experimental investigations.

The choice of normalizations for the figures is, of course, somewhat arbitrary with different choices greatly altering the appearance of the figures. Near the turning points of the steady-state characteristic, the behavior of the functions $\delta I_{\rm inc}/I_{\rm coh}$ and $g^{(2)}(0)-1$ is dominated by the deterministic divergence of the fluctuations, which initially proceeds differently for different mode functions. However, even far from the turning points the normalization can give rise to quite different impressions of the role of the nonuniform cavity mode. For example, with reference to Figs. 1 and 4, the spatially varying field mode has a rather less dramatic effect on the quantity $g^{(2)}(0)-1$ when situations of equal-mean intracavity intensities are compared than when normalizations relative to the respective turning points are employed. On the other hand, the choice of comparing equal X values causes a crossover [Figs. 1(a) and 2, and 4(a), and 5] of a peculiar sort due to the difference in slope of the steady-state curves along the lower branch of the bistability state equation. Further, our choice of equal atomic cooperativity parameters in examining the behavior of $g^{(2)}(0)$ for the various cases is also somewhat arbitrary, since in terms of the ratio $R'=C/C_0$, with C_0 equal to critical cooperativity, the choice $C=40$ (with $\delta=0=\varphi$) corresponds to $R'=10.0$, 4.81, and 8.05 for the plane-wave ring, Gauss-ring, and standing-wave cavities, respectively.

These issues of normalization aside [which in any case do not effect our explicit results (11) and (17)], the linearized coefficients that we have presented can be used to obtain quantitative expressions for the quantum fluctuations of the intracavity field for a wide range of realistic cavity-mode functions by simply substituting the appropriate mode function into Eqs. (11) and (17). Beyond the specific examples of $g^{(2)}(0)-1$ and $\delta I_{\rm inc}/I_{\rm coh}$ that we take in Eqs. (20) and (21), our formalism is readily employed to calculate other effects such as the incoherent spectral density, photon antibunching, and squeezing[12] by making use of appropriate expressions already in the literatures.[1,4,18,19]

ACKNOWLEDGMENTS

This work was supported by the Venture Research Unit of British Petroleum North America and by the National Science Foundation.

[1]L. A. Lugiato, in *Progress in Optics*, edited by E. Wolf (North-Holland, Amsterdam, 1984), Vol. XXI, p. 71.

[2]H. J. Carmichael, *Quantum Statistical Techniques in Quantum Optics* (Springer-Verlag, New York, in press).

[3]P. D. Drummond and D. F. Walls, Phys. Rev. A **23**, 2563 (1981).

[4]M. Gronchi and L. A. Lugiato, Lett. Nuovo Cimento **23**, 593 (1978); G. S. Agarwal, L. M. Narducci, D. H. Feng, and R. Gilmore, Phys. Rev. A **21**, 1029 (1980).

[5]P. D. Drummond, IEEE J. Quantum Electron. **QE—17**, 301 (1981).

[6]H. Haken, *Encyclopedia of Physics* (Springer, Berlin, 1970), Vol. XXV/2C, pp. 60—71 and 153—156.

[7]W. H. Louisell, *Quantum Statistical Properties of Radiation* (Wiley, New York, 1973).

[8]P. D. Drummond and C. W. Gardiner, J. Phys. A **13**, 2353 (1980); P. D. Drummond, C. W. Gardiner, and D. F. Walls, Phys. Rev. A **24**, 914 (1981).

[9]L. Arnold, *Stochastic Differential Equations* (Wiley, New York, 1974); H. Risken, *The Fokker-Planck Equation* (Springer-Verlag, Berlin, 1984).

[10]H. J. Carmichael, J. S. Satchell, and S. Sarkar, Phys. Rev. A **34**, 3166 (1986).

[11]M. Lax, Rev. Mod. Phys. **32**, 25 (1960); C. W. Gardiner, *A Handbook of Stochastic Methods* (Springer, Berlin, 1982).

[12]M. Xiao, H. J. Kimble, and H. J. Carmichael (unpublished).

[13]A. T. Rosenberger, L. A. Orozco, and H. J. Kimble, Phys. Rev. A **28**, 2569 (1983); in *Fluctuations and Sensitivity in Nonequilibrium Systems*, edited by W. Horsthemke and D. Kondepudi (Springer-Verlag, Berlin, 1984), p. 62.

[14]L. A. Lugiato and M. Milani, Z. Phys. B **50**, 171 (1983).

[15]R. J. Ballagh, J. Cooper, M. W. Hamilton, W. J. Sandle, and D. M. Warrington, Opt. Commun. **37**, 143 (1981).

[16]F. Casagrande and L. A. Lugiato, Nuovo Cimento **55B**, 173 (1980).

[17]D. E. Grant and H. J. Kimble, Opt. Lett. **7**, 353 (1982); Opt. Commun. **44**, 415 (1983); H. J. Kimble, P. D. Drummond, D. E. Grant, and A. T. Rosenberger, in *Laser Physics*, Vol. 182 of *Lecture Notes in Physics*, edited by J. D. Harvey and D. F. Walls (Springer-Verlag, Berlin, 1983), p. 14; L. A. Orozco, H. J. Kimble, and A. T. Rosenberger (unpublished).

[18]M. D. Reid and D. F. Walls, Phys. Rev. A **32**, 396 (1985).

[19]M. J. Collett and C. W. Gardiner, Phys. Rev. A **30**, 1386 (1984); C. W. Gardiner and M. J. Collett, *ibid.* **31**, 3761 (1985).